Journal of Food and Drug Analysis

Volume 29 | Issue 2 Article 13

2021

Pepsin-digested chicken-liver hydrolysate attenuates hepatosteatosis by relieving hepatic and peripheral insulin resistance in long-term high-fat dietary habit

ORIGINAL ARTICLE

Pepsin-digested chicken-liver hydrolysate attenuates hepatosteatosis by relieving hepatic and peripheral insulin resistance in long-term high-fat dietary habit

Yi-Hsieng Samuel Wu [a], Yi-Ling Lin [a], Wen-Yuan Yang [b], Sheng-Yao Wang [a], Yi-Chen Chen [a,*]

[a] Department of Animal Science and Technology, National Taiwan University, Taipei, 106, Taiwan
[b] Department of Veterinary Medicine, School of Veterinary Medicine, National Taiwan University, Taipei, 106, Taiwan

Abstract

This study aims to clarify the effects of chicken liver hydrolysates (CLHs) on long-term high-fat diet (HFD)-induced insulin resistance (IR) and hepatosteatosis in mice. *In vitro*, the 400 μM oleic acid (OA)-added medium successfully stimulated the cellular steatosis on FL83B cells, and the cellular steatosis was attenuated ($p < 0.05$) by supplementing with CLHs (4 mg/L). *In vivo*, the effects of CLHs on IR and hepatosteatosis development were tested in 20-week HFD-fed mice. HFD-induced increases in final body weight, but body weight gains of mice were decreased ($p < 0.05$) by supplementing CLHs. Elevated ($p < 0.05$) serum aspartate aminotransferase (AST), alanine transaminase (ALT), alkaline phosphatase (ALP), free fatty acids (FFAs), triglyceride (TG), total cholesterol (TC), and fasted glucose values in HFD-fed mice decreased ($p < 0.05$) by supplementing CLHs. Both results of hepatic steatosis and fibrotic scores also indicated the retardation ($p < 0.05$) of the hepatosteatosis in cotreated groups. Moreover, the CLH supplementation sustained ($p < 0.05$) hepatic and peripheral insulin signal sensitivity in HFD-fed mice. CLH supplementation could ameliorate hepatic lipid deposition, hepatic/peripheral IR in a long-term high-fat dietary habit, and also improve the universal glucose homeostasis by upregulating hepatic and peripheral insulin sensitivities.

Keywords: Adipose tissue, Chicken-liver hydrolysates, Insulin resistance, Non-alcoholic fatty liver disease, Skeletal muscle

1. Introduction

Within decades, broilers have become one of the most acceptable chicken sources compared to local chicken breeds in Taiwan. Their livers are one of the major by-products during the slaughtering process. Generally, their livers are regarded as useless and inexpensive because of their restricted usage. However, livers contain many nutrients, such as proteins, minerals, etc. Thus, a functional ingredient developed from broiler livers may be a practical and potential direction to reduce a handling cost in poultry industry. According to the Council of Agriculture, Executive Yuan, Taiwan, approximately 240.17 million broilers were slaughtered (364,164 metric tons) in 2019 [1]. A liver is approximately 2.5% (w/w) weight in slaughtered broilers. Hence, the annual yield of broiler livers is about 9,000 m.t. in Taiwan. In the previous study, lipogenic gene expressions were significantly downregulated by supplementing with chicken-liver hydrolysates (CLHs); meanwhile, fatty-acid β oxidation were upregulated in high fat/cholesterol diet-fed hamsters supplemented with CLHs [2]. Lin et al. also reported that CLH supplementation could ameliorate the lipid accumulation in livers of alcoholic liquid-diet fed mice [3]. This

Received 15 December 2020; revised 26 March 2021; accepted 31 March 2021.
Available online 15 June 2021.

* Corresponding author. Department of Animal Science and Technology, National Taiwan University, Taipei, 106, Taiwan. Tel: 886-2-33664180; Fax: 886-2-27324070.
E-mail address: ycpchen@ntu.edu.tw (Y.-C. Chen).

https://doi.org/10.38212/2224-6614.3351

hepatoprotection of CLHs against alcoholic damage has been patented in the USA as well [4].

Annually, 4.2 million people die from diabetes mellitus (DM) associated complications worldwide, and 90% of them relate to type 2 DM (T2DM) [5]. Remarkably, more than 70% of T2DM patients are diagnosed with non-alcoholic fatty liver disease (NAFLD), which means a high association between them [6, 7]. Furthermore, it is suggested that NAFLD patients should be screened for T2DM [8]. Hence, the studies on delaying IR occurrence or improving insulin sensitivity are valuable to NAFLD therapy and T2DM. Recently, many food-origin compounds and protein hydrolysates have been attracted increasing attention due to its various bio-activities [9-11]. Besides, lysine and glycine supplementation sustain the blood glucose homeostasis in streptozotocin-induced hyperglycemic rats [12, 13]. For hyperglycemia-induced hippocampus damages, taurine could interfere with the advanced glycation end products formation *in vivo* [14]. Notably, a dietary leucine effectively ameliorated the IR, tissue inflammation, and hepatic lipid deposition; furthermore, the synergistic effects of leucine and some anti-diabetic agents have also been reported [15]. Besides, previous studies reported that the decreased hepatic lipid deposition against an excessive energy intake could highly correlate to the balance of triglyceride (TG) synthesis and energy expenditure (fatty-acid β oxidation), which are both modulated by up-streaming insulin signal, thus emphasizing the crucial role of IR in NAFLD [16, 17]. Furthermore, diacylglycerol o-acyltransferase 2 (DGAT2), the last major enzyme for converting diacylglycerol to triacylglycerol, and the medium-chain specific acyl-CoA dehydrogenase (ACADM), a crucial enzyme in fatty-acid β oxidation, are suitable markers for screening the potential hepatoprotective agent against NAFLD.

Although the lipid-lowering effects of this patented CLH has been proven via a hamster model, the effects of this CLH on the insulin signaling in a long-term high-fat dietary habit are still not elucidated [2]. Chang et al. report that valproic acid enhances the hepatocyte steatosis via the FL83B cell model. This cell model is suitable for screening the effects on hepatocellular lipid accumulation [18]. Besides, unlike other animal models, a long-term high-fat diet (HFD) feeding mimics both the histopathology and pathogenesis of human NAFLD and sheds light on the clinical application [19]. In this study, we would like to clarify the lipid-lowering mechanism of CLHs on hepatocytes via the FL83B-cell model, as well as understand if CLHs could improve the glycemic homeostasis in long-term HFD-fed mice. This study also aims to clarify the hepatoprotective effects of CLHs on long-term HFD-induced IR in mice. It offers important evidence to support its potential application to those NAFLD patients with pre-diabetic symptoms in the future.

2. Materials and methods

2.1. Materials and chemicals

All boiler livers (Arbor Acres^{+}) used in this study were purchased from Charming Food Intl. Marketing Co., Ltd. (Taichung, Taiwan). This company has the Certified Agricultural Standards (CAS) certification in Taiwan. The transportation, storage, and manufacture of chicken-liver hydrolysates (CLHs) were conducted according to our patent [4]. All other chemicals used in this study are of analytical grade.

2.2. Nutritional composition and free amino-acid profile/Imidazole-ring dipeptides of CLHs

The nutritional composition of CLHs (i.e., water, crude fat, crude protein, and ash contents) was analyzed according to the assays of the Association of Official Analytical Chemists (AOAC) [20]. For the free amino-acid profile, anserine and carnosine in CLHs were analyzed according to a previous study by using an Amino Acid Analyzer (Hitachi L8800 Amino Acid Analyzer, Hitachi High-Technologies Co., Tokyo, Japan) in the Food Industry Research and Development Institute (Hsinchu City, Taiwan) [3].

2.3. FL83B cell culture

First, the culture method of FL83B cells was slightly modified from the American Type Culture Collection (ATCC) [18]. The short- and long-term impacts of CLHs on the survivability of FL83B cells in fetal bovine serum (FBS) containing culture system were determined (Fig. 1A), which could monitor cellular morphology and growth condition compared to those of ATCC. Survival assay (Cell Counting Kit-8; Enzo Life Science, Inc., Farmingdale, NY, USA) and lactate dehydrogenase

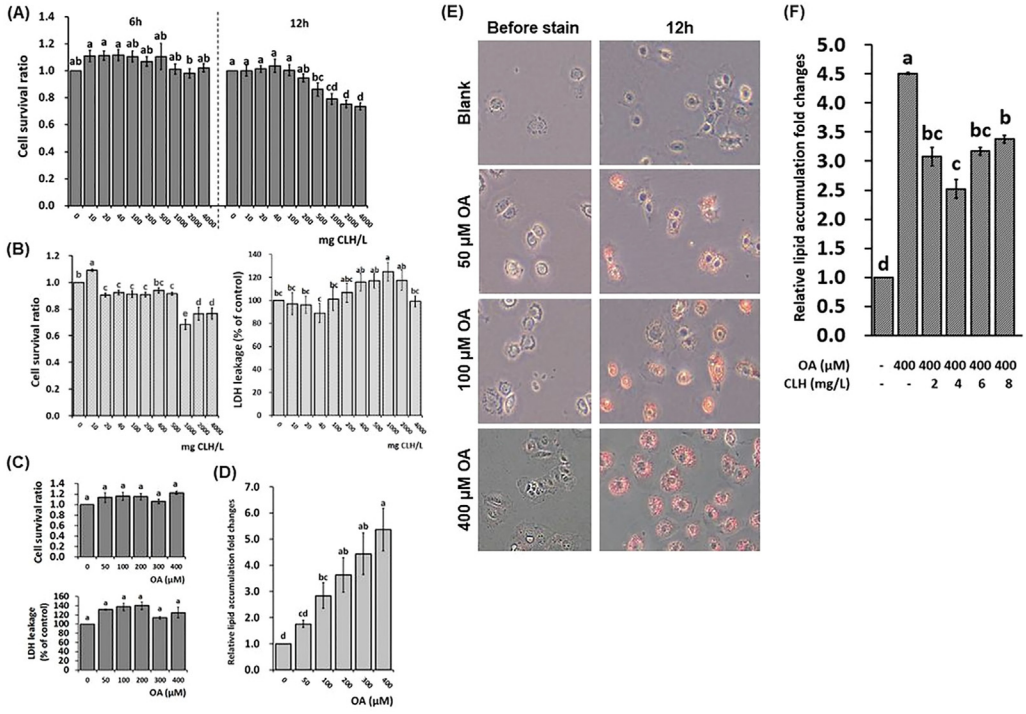

Fig. 1. Cell survival assay, lactic acid dehydrogenase (LDH) leakage assay, and lipid accumulated model of FL83B cells. (A) Cell survival assay under different chicken liver hydrolysate (CLH) concentrations on 6- and 12-h incubation, respectively. (B) Cell survival and LDH leakage assays under different CLH concentrations. (C) Cell survival and LDH leakage assays under different OA concentrations. (D) Lipid content analysis of FL83B cells by using Nile red stain under different OA concentrations. The cultural conditions were as stated above in part (B). (E) Lipid stain by using Oil Red O stain under different OA concentrations. (F) Lipid content analysis of FL83B cells treated with 400 μM OA and different CLH concentrations by using Nile red stain. The data are given as mean ± SEM (n = 6). In part (A), data bars without a common letter in 6-h and 12-h incubation, respectively, indicate a significant difference ($p < 0.05$). In contrast, the other data bars in each test parameter without a common letter indicate a significant difference ($p < 0.05$). Each value of the treatment was adjusted with its control. In part (A), the assay was based on the ATCC's cultural guideline (F12K medium with 10% FBS). Other assays were based on the F12K medium without FBS under 12-h incubation.

(LDH) leakage assay (LDH-Cytotoxicity Colorimetric Assay Kit II; BioVision Inc., Milpitas, CA, USA) of cells were conducted according to the commercial manuals, respectively. FL83B cells were seeded in a 96-well plate (20,000 cells/well), incubated for 12 h to attach. The cell survival assay was then taken after another 6- or 12-h incubation under 100 μL 10% FBS-contained media (0 to 4000 mg CLHs/L). Next, 4 h before the harvest time point, the 10 μL CCK-8 was added. Final optical density values were obtained via Synergy H1 Hybrid Reader (Bio-Tek Instruments, Inc., Winooski, VT, USA).

2.4. Lipid accumulation model of the FL83B cell

According to the previous study, the lipid accumulation model was developed, and 12 h for oleic acid (OA)-induction was proved to induce the cellular steatosis successfully [18]. Thus, the 12 h-incubation was chosen in the following procedure. The CCK-8 cell survival assay and LDH leakage analysis were conducted for determining the optimal concentration of OA in the treating medium. The FL83B cells were seeded in a 96-well plate (20,000 cells/well) and incubated for 12 h for attachment both in CCK-8 and LDH assays. The cell survival assay was taken after a 12 h incubation under the 100 μL treating medium. 10 μL CCK-8 solution was added at 4 h before the harvest time point. In LDH leakage analysis, the medium was harvested and measured after a further 12 h incubation. Besides, both of the two experiments were based on the F12K medium without FBS to elevate the cellular accessibility of OA [18]. For visual analysis, the procedure of Oil red O stain was conducted respectively. The FL83B cells were seeded in

a 12-well plate (20,000 cells/well) and incubated for 12 h to attach. Next, the assay was taken after the further 12-h incubation under the one mL treating medium. The medium was based on the FBS free F12K medium. 4% paraformaldehyde and Oil red O solution (0.35 g in 100 mL 60% isopropanol) was used to fix and stain cells for 10 min, sequentially. The magnification of all images was 200 ×. The cellular lipids were illustrated in bright red in the photos. The microscopic analysis was determined via Olympus microscope (Olympus Co., Tokyo, Japan) with Toup View 3.7 software (Toup Tek Co., LTD, Hangzhou, China). The Nile red stain method was used (excitation: 485 nm, emission: 535 nm) [18]. FL83B cells were seeded in 20,000 cells per well of 96-well plate and incubated at 37 °C, 5% CO_2 for 12 h. All treating intervals were 12 h. All values were adjusted with each fluorescent intensity of Hoechst stain (excitation: 350 nm, emission: 461 nm), indicating nuclei. The lipid content was calibrated with those of the control group (0 μM OA).

2.5. Western blotting

Protein from FL83B cells was extracted by RIPA buffer (Merck & Co., Inc., Kenilworth, NJ, USA), and samples were then mixed with Laemmli buffer and boiled at 95°C for 10 min. The 10% homogenates of tissue samples were also made with RIPA lysis buffer (Merck & Co.) with proteinase inhibitor cocktail (cOmplete™, mini, EDTA-free Protease inhibitor cocktail, Roche, Basel, Switzerland) via MiniBeadBeater-16 (BioSpec Products Inc., Bartlesville, OK, USA). The following procedure was done as described in Chang et al [18]. Densitometry analyses were performed by using Image Lab software

Table 1. Growth performance, organ and fat-pad weights, serum biochemical values, hepatic antioxidative capacity, and hepatic pro-inflammatory cytokines of experimental mice.

	Control	CLH	HFD	HFD + CLHL	HFD + CLHH
Growth performance					
Initial body weight (g)	25.32 ± 0.56a	25.66 ± 0.61a	25.48 ± 0.86a	25.29 ± 0.76a	24.54 ± 0.71a
Final body weight (g)	36.21 ± 1.48c	36.88 ± 0.63c	53.30 ± 0.80a	49.44 ± 1.12b	48.48 ± 0.72b
Body weight gain (g)	10.89 ± 0.99c	11.22 ± 0.48c	27.82 ± 0.71a	24.14 ± 0.48b	23.94 ± 0.46b
Feed intake (g/mouse/day)	2.23 ± 0.03b	2.32 ± 0.03a	1.95 ± 0.01c	1.92 ± 0.04c	1.93 ± 0.02c
Water intake (mL/mouse/day)	4.42 ± 0.19a	4.24 ± 0.12a	3.37 ± 0.10b	3.56 ± 0.02b	3.70 ± 0.10b
Energy intake (kcal/mouse/day)	8.58 ± 0.13c	8.94 ± 0.12bc	9.43 ± 0.03a	9.30 ± 0.19ab	9.36 ± 0.10a
Feed efficiency (g WG/g diet)	0.04 ± 0.00c	0.04 ± 0.00c	0.11 ± 0.00a	0.09 ± 0.00b	0.09 ± 0.00b
Organ weights					
Heart (g)	0.17 ± 0.01a	0.17 ± 0.01a	0.17 ± 0.00a	0.17 ± 0.01a	0.17 ± 0.01a
Liver (g)	1.28 ± 0.05b	1.27 ± 0.02b	1.97 ± 0.17a	1.60 ± 0.20ab	1.51 ± 0.10b
Kidney (g)	0.33 ± 0.01b	0.33 ± 0.00b	0.36 ± 0.01a	0.36 ± 0.01a	0.36 ± 0.01a
Abdominal fat (g)	2.23 ± 0.10b	2.37 ± 0.19b	4.09 ± 0.13a	4.02 ± 0.14a	4.17 ± 0.26a
Blood biochemical values					
TG (mg/dL)	172.63 ± 17.14c	173.88 ± 5.20c	322.38 ± 16.79a	231.00 ± 25.60b	245.50 ± 17.94b
TC (mg/dL)	187.38 ± 10.64b	197.63 ± 6.89b	271.25 ± 23.84a	216.38 ± 27.42ab	198.38 ± 23.72b
AST (U/L)	97.50 ± 6.13c	79.00 ± 4.09c	159.63 ± 9.84a	136.88 ± 4.98ab	126.00 ± 14.24b
ALT (U/L)	51.50 ± 4.00bc	44.88 ± 2.42c	103.38 ± 18.84a	77.38 ± 11.51ab	64.63 ± 7.44bc
ALP (U/L)	299.50 ± 4.26b	297.13 ± 2.80b	319.63 ± 3.01a	272.63 ± 3.28c	248.88 ± 7.72d
Albumin (g/dL)	3.21 ± 0.06a	3.24 ± 0.05a	3.16 ± 0.06a	3.18 ± 0.04a	3.11 ± 0.08a
Ketone body (mg/dL)	6.22 ± 0.20b	6.86 ± 0.03a	6.15 ± 0.16b	6.28 ± 0.17b	6.47 ± 0.11ab
Fasted glucose (mg/dL)	126.00 ± 4.44d	135.00 ± 3.25cd	184.13 ± 8.23a	152.63 ± 7.27bc	171.88 ± 12.61ab
Free fatty acid (mmol/L)	0.55 ± 0.02d	0.92 ± 0.02b	1.13 ± 0.01a	0.80 ± 0.05c	0.80 ± 0.03c
Hepatic antioxidative capacities					
TBARS (nmole MDA eq./mg protein)	0.88 ± 0.02b	0.70 ± 0.04b	1.47 ± 0.13a	0.78 ± 0.05b	0.73 ± 0.04b
Reduced GSH (nmole/mg protein)	26.29 ± 1.46a	29.41 ± 1.42a	29.08 ± 1.99a	28.41 ± 2.15a	29.38 ± 3.34a
TEAC (nmole/mg protein)	127.72 ± 2.17ab	136.68 ± 7.25a	110.62 ± 2.64c	121.76 ± 3.27bc	117.34 ± 1.76bc
SOD (unit/mg protein)	6.51 ± 0.22b	8.74 ± 0.16a	2.70 ± 0.32d	4.75 ± 0.48c	5.43 ± 0.31c
CAT (unit/mg protein)	36.33 ± 3.75ab	29.76 ± 1.55abc	28.00 ± 1.84c	36.43 ± 2.72a	29.37 ± 1.68bc
GPx (unit/mg protein)	26.20 ± 1.60a	26.55 ± 1.42a	16.34 ± 1.30b	25.35 ± 0.99a	23.11 ± 2.66a
Hepatic pro-inflammatory cytokines					
TNF-α (pg/mg protein)	16.35 ± 0.91c	20.56 ± 0.88bc	35.37 ± 3.07a	20.52 ± 1.67bc	25.19 ± 2.26b
IL-1β (pg/mg protein)	131.95 ± 7.03b	123.74 ± 7.18b	200.28 ± 12.36a	139.42 ± 7.69b	121.95 ± 11.75b

*The data are given as mean ± SEM (n = 8, except feed, water, and energy intake, and feed efficiency, n = 4). Mean values in each test parameter without a common letter are significantly different ($p < 0.05$).

**All mice were randomly assigned to one of following groups: (1) Control group: basal diet; (2) CLH group: basal diet and CLHs; (3) HFD group, high-fat diet (HFD, fat: 46.5% of caloric); (4) HFD + CLHL group: HFD and CLHs (appr. 170 mg/kg BW); (5) HFD + CLHH group: HFD and CLHs (appr. 510 mg/kg BW).

(BioRad). The relative optical density of protein bands was normalized with the β-Tubulin band. The information of antibodies used in this study was shown in Suppl. Table 1.

2.6. Animals and diets

The animal use and protocol were reviewed and approved by the National Taiwan University Care Committee (IACUC No.: NTU106-EL-00093). Forty male 8-week-old C57BL/6 mice were purchased from the Laboratory Animal Center of National Taiwan University. The animal house's environmental parameters were as follows: temperature, 22 ± 2°C, and light/dark cycle, 12/12 h. All mice were randomly assigned to one of the following groups (n = 8 per group): (1) Control group: basal diet; (2) CLH group: basal diet and CLHs; (3) HFD group, high-fat diet (HFD, fat: 46.5% of caloric); (4) HFD + CLHL group: HFD and CLHs (appr. 170 mg/kg BW); (5) HFD + CLHH group: HFD and CLHs (appr. 510 mg/kg BW). Two mice with an ear-tag (NO. 1 or 2) were housed in one cage. The AIN-93M formula-based diet was prepared and served, and CLHs were mixed with basal feed ingredients according to our previous study within the 20-week experimental period [21].

2.7. Collection of serum, liver, abdominal fat, feces, and muscle of experimental mice

Blood was collected from each mouse at the end of the experiment. At the end of the investigation, all mice were weighed and fasted for 8 h and then sacrificed by CO_2 asphyxiation. Blood samples were collected by orbital sinus and kept at room temperature for one h. Sera were obtained after centrifugation (Model# 3700, Kubota Co., Tokyo, Japan) at 3000×*g* and 4°C for 10 min. The organ tissues of each mouse were removed, weighed, and recorded individually. The one-third dominant lobe of the liver of each mouse was placed into a 10% formaldehyde solution for histological analyses, and other remnants, peri-renal adipose tissues, and right or left hindlimb skeletal muscle from thigh to ankle were immediately immersed in liquid N_2 and then stored at −80°C for the following analyses.

2.8. Serum biochemical values and lipid profiles of livers and feces

Serum TG, TC, aspartate aminotransferase (AST), ALT, alkaline phosphatase (ALP), albumin, ketone body (KB), FFA, and fasted glucose was assayed by using an auto biochemistry analyzer (TBA 120FR TOSHIBA Chemistry Analyzer, Toshiba Technology, Tokyo, Japan) and their corresponding kits. Liver and fecal lipids were extracted according to the previous study [22]. The Folch's extraction procedure was used, and the extracts were dried under N_2 and resuspended in isopropanol. Overall, TC and TG concentrations were measured by using commercial kits (Randox Laboratories Ltd., Antrim, UK).

2.9. Hepatic lipid peroxidation and pro-inflammatory cytokine levels

Hepatic levels of thiobarbituric acid reactive substance (TBARS), reduced glutathione (GSH), and trolox equivalent antioxidative capacity (TEAC), as well as superoxide dismutase (SOD), catalase (CAT), and glutathione peroxidase (GPx) activities were assayed according to previously described methods from Chen et al [23]. The hepatic tumor necrosis factor (TNF)-α and interleukin (IL)-1β levels were measured using an enzyme-linked immunosorbent assay (ELISA) and conducted according to the commercial manufacturer's instructions (TNF-α, BioLegend, Inc., San Diego, CA, USA; IL-1β, R&D system, Minneapolis, MN, USA).

2.10. Histological analyses and immunohistochemistry stain of livers

All tissue blocks, slides, and stains (H&E and Sirius red stain) were prepared according to the methods described in our previous study [23]. The blank liver slides were divided according to the number of the ear tag in each cage (NO. 1 and NO. 2). In contrast, immunohistochemistry stain (IHC) and Sirius red stains of livers were conducted with those of NO. 1 and NO. 2 mice per cage, respectively. However, the analysis was observed and graded via a visual inspection by the veterinarian based on a report by Dixon, Bhathal, Hughes, and O'Brien [24]. The quantification of redness in Sirus red-stained slides of the liver tissue (40×) was also analyzed using ImageJ (National Institutes of Health, Bethesda, MD, USA). The minimum and maximum thresholds were given as 145/168. For an IHC analysis, the heat-induced epitope retrieval was conducted, and tissue sections were incubated with hydrogen peroxide block (TA-060-HP; ThermoFisher, Waltham, MA, USA) and protein block solution (TA-060-PBQ; ThermoFisher). Primary

antibody DGAT2 (ab237613, Abcam; 100 × dilution) and ACDAM (ab92461, Abcam; 100 × dilution) were used for 40 min incubation in a humidified chamber. Next, tissue sections were treated with rabbit antibody enhancer (D39; Golden Bridge International, Inc., Bothell, WA, USA) and polymer-HRP for rabbit (D39; Golden Bridge International, Inc.), respectively. The DAB peroxidase substrate (TA-060-QHSX and TA-002-QHCX; ThermoFisher) was used. The microscopic analysis was conducted via Leica DM500 microscope (Leica Microscope, Singapore) with Toup View 3.7 software (Toup Tek Co., LTD, Hangzhou, China).

2.11. Intraperitoneal glucose tolerance test

The intraperitoneal glucose tolerance test (ipGTT) was conducted in the 20th week of the experimental period. All mice were fasted for 8 h before a glucose (2 g/kg BW) intraperitoneal injection. Then blood samples were collected via the facial vein sampling method. The sensitivity of blood glucose monitor (GM300, Bionime Corp., Taichung, Taiwan) is from 10 to 600 mg/dL. The area under the curve (AUC) was calculated from the sampling period of 0 to 120 min. The procedure was according to Andrikopoulos et al. [25].

2.12. Statistical analysis

The experiment was conducted by using a completely randomized design. When a significant difference ($p < 0.05$) among groups was detected using the one-way analysis of variance (ANOVA), differences between treatments were further distinguished using the least significant difference (LSD) test. All statistical analyses of data were conducted via SAS (SAS Institute Inc., Cary, NC, USA, 2002).

3. Results

3.1. Effects of CLHs on OA-induced lipid accumulation in vitro

The short- and long-term impacts of CLHs on the survivability of FL83B cells in FBS containing culture system were determined (Fig. 1A). There were almost no differences among tested CLH levels for 6 h; on the contrary, the cell survival ratio for 12-h treatment in the FBS culture system was decreased ($p < 0.05$) beyond 500 mg CLH/L. Because the OA 12-h incubation was successfully proven to enhance cellular steatosis, the 12-h incubation was chosen in the following procedure. Next, the optimal concentration range of CLHs or OA used in the following assays were determined in the FBS-free culture

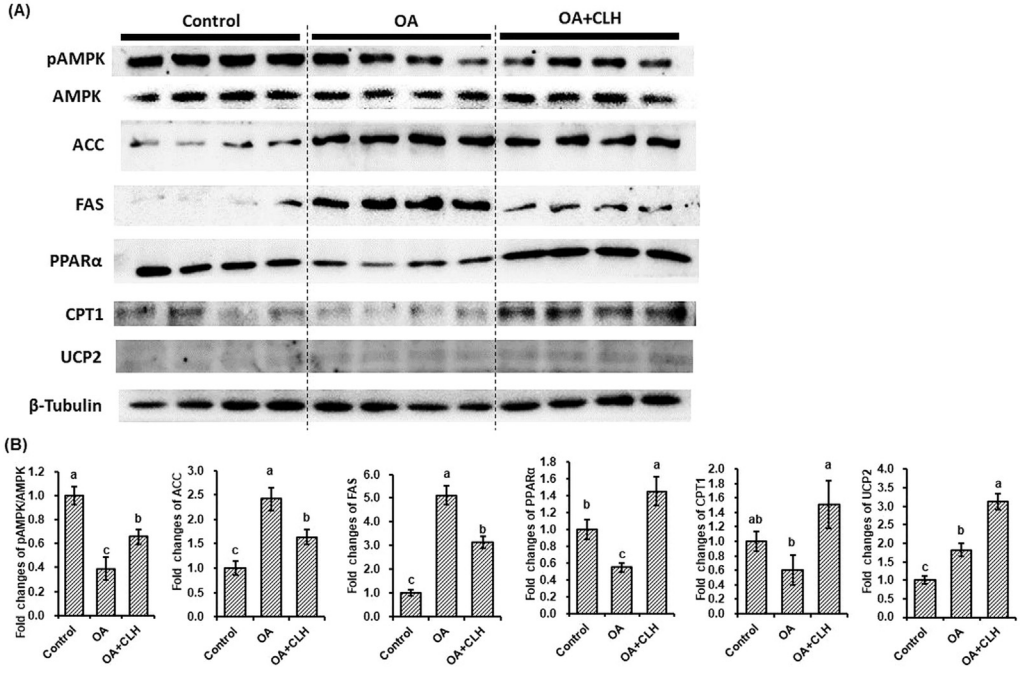

Fig. 2. Effects of CLHs on target protein expressions in the OA-induced FL83B cells. (A) The illustration of protein expressions related to fatty-acid synthesis (pAMPK/AMPK, ACC, and FAS) and energy expenditure (PPARα, CPT1, and UCP2) under OA and CLH intervention. (B) The quantification results of western blotting, including proteins related to fatty acid synthesis and energy expenditure. The data are given as mean ± SEM (n = 8). Data bars in each target protein without a common letter are significantly different ($p < 0.05$).

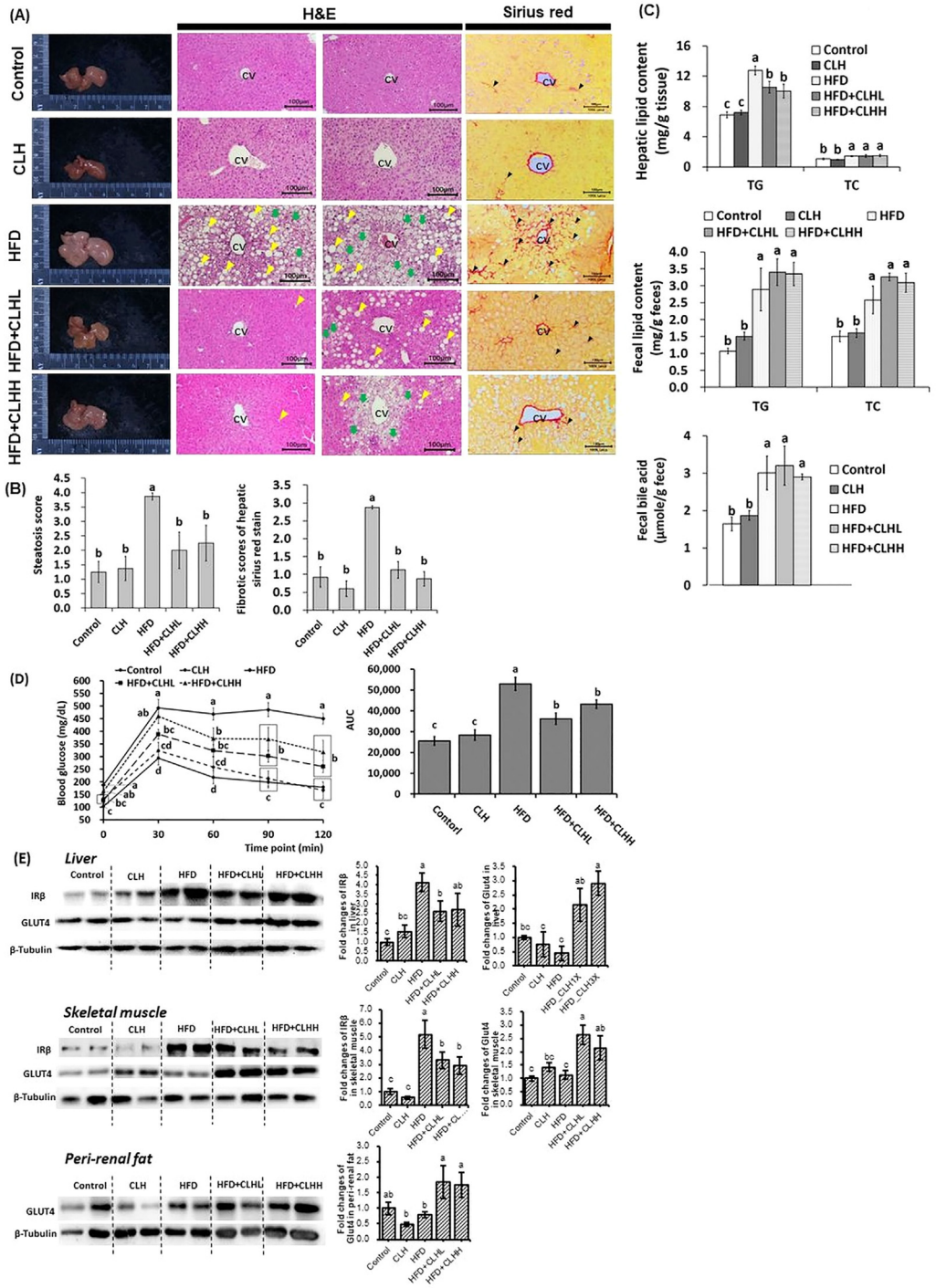

Fig. 3. The pathohistological analyses in liver tissues, hepatic lipid, fecal lipid/bile acid profiles, ipGTT, and protein expressions in the liver, skeletal muscle, and peri-renal fat tissues of experimental mice. (A) Appearances, and H&E and Sirius red stain of liver tissues were shown. The histological photomicrographs were displayed with 100 × magnification. The scale bar was established in the bottom right corner of each image. The yellow and green arrowheads indicate macrosteatosis and microsteatosis, respectively, and the black arrowheads indicate the fibrotic scar. CV means a central vein. (B) The quantification was conducted via the respective histological grading system. The data are given as mean ± SEM (n = 8 for H&E stain; n = 4 for Sirius red stain). Data bars in steatosis or fibrotic scores without a common letter are significantly different ($p < 0.05$). (C) Hepatic lipid and fecal lipid/bile acid of experimental mice at the end of the experiment. The data are given as mean ± SEM (n = 8). Data bars in each test parameter without a common letter are significantly different ($p < 0.05$). (D) The glucose tolerance test was conducted via intraperitoneal injection. The AUC was calculated, and the results were shown via the bar chart. Data are given as mean ± SEM (n = 8). Data points of each time point and bars of AUC without a common letter are significantly different, respectively ($p < 0.05$). (E) The illustration and quantification of proteins related to insulin signals in the liver, skeletal muscle, and peri-renal fat tissues, respectively. The data are given as mean ± SEM (n = 8). Data bars in each target protein without a common letter are significantly different ($p < 0.05$).

system. The cell survival ratio was increased ($p < 0.05$) under 10 mg CLH/L addition but decreased ($p < 0.05$) since an addition was higher than 20 mg CLH/L (Fig. 1B). Meanwhile, the cellular LDH leakage was elevated ($p < 0.05$) beyond 1,000 mg CLH/L addition (Fig. 1B). Besides, no ($p > 0.05$) differences in either cell survival ratio or LDH leakage were detected under the tested OA concentrations (0 to 400 μM, Fig. 1C). Fig. 1D showed that the intracellular lipid accumulation was significantly induced ($p < 0.05$), while OA concentration exceeded 100 μM. More lipid accumulation was observed in the 400 μM OA induction via the Oil red O stain (Fig. 1E). Furthermore, an increase of cellular lipid accumulation by a 400 μM-OA induction was attenuated ($p > 0.05$) by CLH treatments, and the largest reduction was shown at 4 mg CLH/L addition (Fig. 1F). According to the protein expressions related to fatty-acid synthesis and fatty-acid β oxidation (Fig. 2B), the downregulations ($p < 0.05$) of AMP-activated protein kinase phosphorylation (pAMPK/AMPK), peroxisome proliferator-activated receptor α (PPARα), and carnitine palmitoyltransferase 1 (CPT1), as well as upregulations ($p < 0.05$) of acetyl-CoA carboxylase (ACC), fatty acid synthase (FAS), and uncoupling protein 2 (UCP2) were assayed in the OA induction. However, the decrease of pAMPK/AMPK, as well as increases of ACC and FAS expressions by OA induction, were reversed ($p < 0.05$) by CLH treatment; meanwhile, PPARα, CPT1, and UCP2 expressions were upregulated ($p < 0.05$) (Fig. 2B).

3.2. Effects of CLHs on physiological parameters, blood biochemical values, hepatic antioxidative capacities, and pro-inflammatory cytokines of experimental mice

Increased final body weights, body weight gains, and feed efficiencies by the HFD feeding were decreased ($p < 0.05$) by CLH supplementation, but there was no ($p > 0.05$) difference in feed intakes among HFD and CLH-cotreated groups (HFD + CLHL and HFD + CLHH groups) (Table 1). Regarding blood biochemical values (Table 1), serum TG, TC, FFA, AST, ALT, and ALP were elevated ($p < 0.05$) under the HFD feeding but amended ($p < 0.05$) by supplementing with CLHs. Serum albumin levels were not ($p > 0.05$) influenced. Still, the serum ketone body (KB) of the CLH group was higher ($p < 0.05$) than that of other groups. Liver TBARS values in the HFD group were higher ($p < 0.05$) than those of control diet-fed groups (Control and CLH groups) but decreased ($p < 0.05$) in CLH cotreated mice. Although there were no ($p > 0.05$) difference in reduced GSH contents in livers among groups, liver TEAC values, and SOD, CAT, and GPx activities in the HFD group were lower ($p < 0.05$) than those of control diet-fed groups. However, those values in HFD-fed mice were strengthened ($p < 0.05$) by CLH intervention. Furthermore, the higher ($p < 0.05$) hepatic pro-inflammatory cytokines (TNF-α and IL-1β) due to the HFD feeding were improved ($p < 0.05$) by supplementing with CLHs.

3.3. Effects of CLHs on hepatic steatosis and insulin resistance of liver, adipose tissue, and skeletal muscle

Results of H&E stains revealed the morphology of hepatosteatosis in livers of HFD-fed mice and fewer lipid droplets in CLH cotreated mice (Fig. 3A). Similarly, the steatosis score of the HFD group was higher ($p < 0.05$) than that of other groups (Fig. 3B), and the HFD-induced increases of liver TG contents were also decreased by supplementing with CLHs ($p < 0.05$; Fig. 3C). Increased ($p < 0.05$) fecal lipid and bile-acid contents were measured in HFD-fed mice than control-diet fed mice, but there were tendencies toward higher fecal TG and TC contents in CLH cotreated groups rather than HFD group (Fig. 3C). Furthermore, Sirius red-stained photos indicated that the more fibrotic scars in livers of HFD-fed mice were diminished by supplementing with CLHs (Fig. 3A). The results of fibrotic scores were corresponding to them (Fig. 3B). According to Fig. 3D, the blood glucose levels of the HFD group were the highest ($p < 0.05$) from 30 to 120 min after a glucose i.p. injection among groups, and the increased ($p < 0.05$) AUC of HFD-fed mice was decreased ($p < 0.05$) by supplementing with CLHs. Similarly, the higher ($p < 0.05$) fasted serum glucose values of HFD-fed mice were observed than those of control-diet fed mice but decreased by supplementing with CLHs (HFD + CLHL vs. HFD, $p < 0.05$) (Table 1). The protein expressions of insulin receptor β (IRβ) in both liver and skeletal muscle were upregulated ($p < 0.05$) by the HFD feeding but downregulated ($p < 0.05$) by supplementing with CLHs (Fig. 3E). Regarding the glucose transportation in the organs (Fig. 3E), no ($p < 0.05$) differences of Glucose transporter type 4 (GLUT4) protein expressions in the liver, skeletal muscle, and peri-renal fat tissues among the HFD group and control-diet fed groups, but GLUT4

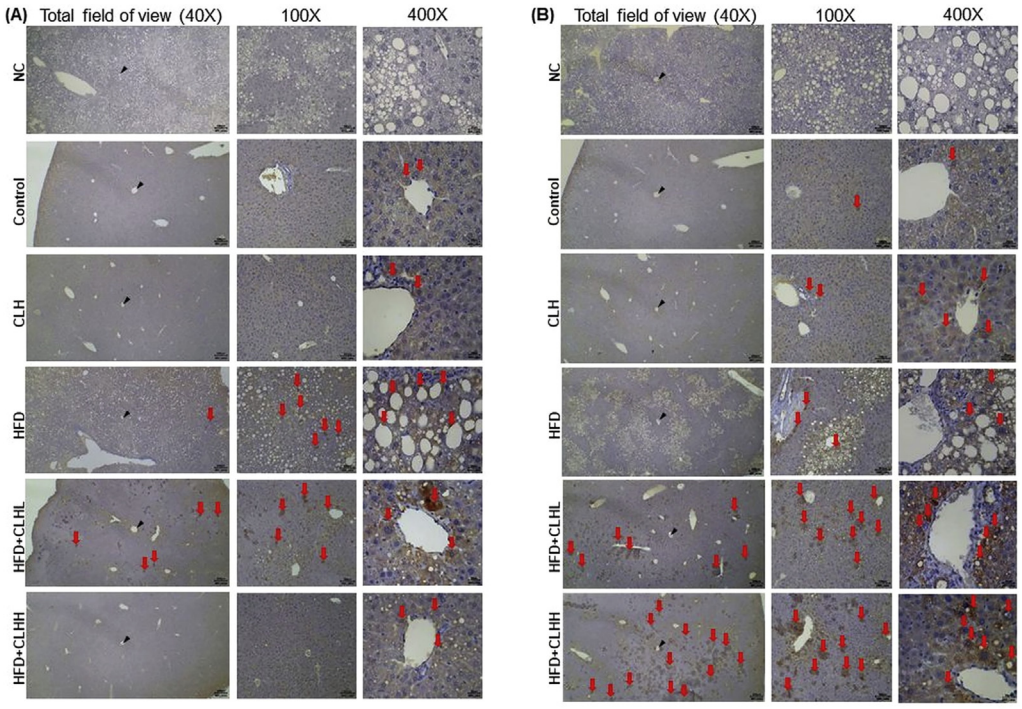

Fig. 4. Immunohistochemical analyses in the liver of experimental mice. (A) DGAT2 and (B) ACADM protein expressions were IHC analyzed. DGAT2 is the last major enzyme for converting diacylglycerol to TG; whereas, ACADM is the crucial enzyme in fatty-acid β oxidation. Histological photomicrographs were shown at 40 × , 100 × , and 400 × magnifications, respectively. The red arrows indicate a positive area, while the black arrowheads indicate the central vein (CV). Liver sections were examined with primary antibody (except negative control, NC) and hematoxylin stained.

expressions in HFD-fed mice were increased ($p < 0.05$) multiple times via supplementing with CLHs (Fig. 3E). Next, the HFD feeding resulted in more DGAT2 protein expressions in livers; however, CLH supplementation diminished the positively stained area (Fig. 4A). Besides, the CLH-induced increase of ACADM protein amounts was observed in HFD cotreated mice rather than those without CLHs (Fig. 4B).

4. Discussion

According to the proximate analysis of CLHs, the major components were 69.57% protein and 22.93% ash (Suppl. Table 2). There were many kinds of free amino acids and anserine (imidazole-ring dipeptide) in CLHs [e.g., L-lysine, branched-chain amino acids [BCAAs, valine (Val), leucine (Leu), and isoleucine (Ile)], β-alanine (a precursor of carnosine), L-aspartic acid, glycine, L-ornithine, taurine, and anserine] (Suppl. Table 2). Moreover, the amount of BCAAs (1800 mg/100g CLHs) was consistent in CLHs to be regarded as the quality control index for further CLH manufacturing.

The *in vitro* experiment was designed to simulate the long-term HFD exposure, and the cell model of the OA-induced hepatocyte steatosis which could interpret the *in vivo* findings was well built [9, 16, 26]. According to D'Antona et al., plasma peak concentrations after a bolus administration of isoleucine, leucine, and valine were revealed as 750, 2000, and 1800 pmole/μL, respectively, and the value was helpful to determine the physiological meanings in a cell model [27]. After conversion, the 40 mg CLHs (Ile, Leu, and Val were 380.54, 831.75, and 626.49 mg/100g CLHs, Suppl. Table 2) in a one-L medium would simulate the portal vein BCAA concentration above proximately. However, the cytotoxicity of CLHs was low because survival ratios of FL83B cells were still about 80% even though the treating concentrations were 100 times (4000 mg CLHs/L) than *in vivo* concentration reference (40 mg CLHs/L eq.) (Fig. 1A). Moreover, Fig. 1F indicated that the effective treating concentration of CLHs at 2 to 8 mg/L could decrease the lipid accumulation in OA-treated FL83B cells. It was less than the *in vivo* concentration reference (40 mg CLHs/L eq.). Therefore, the effects of CLHs was not only nutritional but also bio-functional. The lipid droplets were found under OA treatment, and the protein expression pattern of fatty-acid synthesis (ACC and FAS) was consistent with

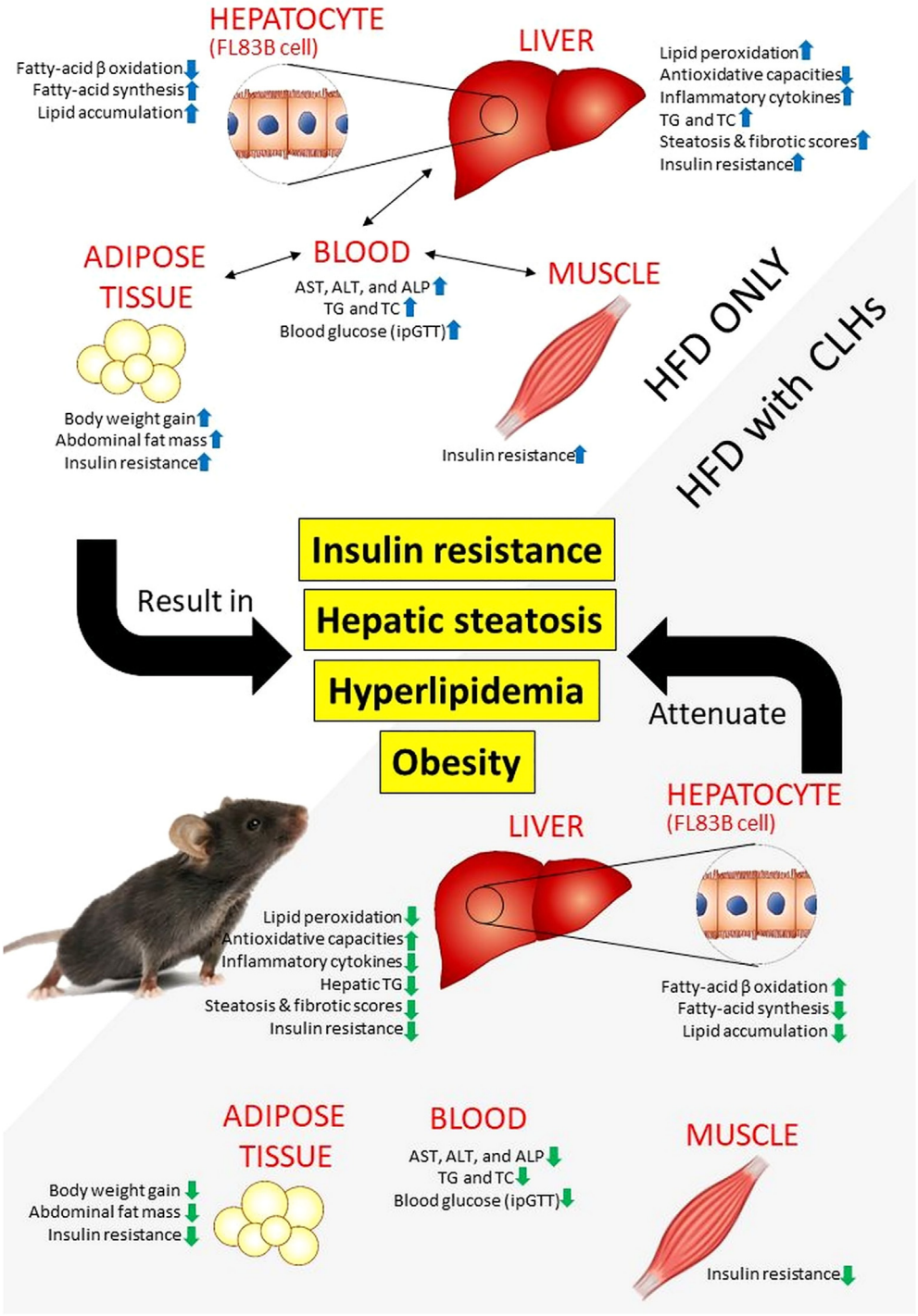

Fig. 5. The ameliorative effects of CLHs on insulin resistance, hepatic steatosis, hyperlipidemia, and obesity against a chronic HFD induction. The HFD-induced metabolic disorders are indicated in the white zone. At the same time, the ameliorative effects of CLHs are shown in a grey zone.

the previous *in vivo* study (Fig. 2) [18]. The protein regulating pattern results showed that CLHs could attenuate the cellular steatosis directly via down-regulating fatty-acid synthesis and upregulating energy expenditure (Fig. 2). Moreover, the phosphorylation of AMPK, the upstream messenger of cellular energy metabolism, was significantly increased in this study (Fig. 2), which contributed

to its downstream signal cascades [28]. Besides, the AMPK activation improved hepatic steatosis in most NAFLD studies [25, 29, 30].

The bio-functionalities of CLHs had been proven due to BCAAs, taurine, acidic amino acid, and anserine [2, 3, 21, 23, 30]. In this study, the CLHs could decrease ($p < 0.05$) body weight gains against the long-term HFD (fat: 46.5 kcal%) induction in mice (Table 1). In comparison with the previous results, the disparity in those regulating patterns could be due to the difference in the period of HFD-feeding intention (8 weeks vs. 20 weeks) and rodent species (hamsters vs. mice). Remarkably, the hypolipidemic effects of CLHs were consistent (Table 1) [2]. Regarding enhancing antioxidant capacities of HFD-fed mice cotreated with CLHs (Table 1), the antioxidant effects of CLH supplementation might be attributed to imidazole ring molecules, β-alanine, hydrophobic amino acids, and antioxidant minerals [31]. Moreover, the ameliorative effects of CLHs on increased liver weights, pro-inflammatory cytokines (TNF-α and IL-1β), and worse hepato-pathological analyses HFD-fed mice were remarkable (Table 1 & Fig. 3). There were 7/8 highly severe and 1/8 severe in the HFD group, while only 3/8 highly severe in the CLH-cotreated group (Suppl. Table 3), which showed the pathohistological improvement under the CLH intervention. Both results of hepatic steatosis and fibrotic scores apparently indicated the delay of the hepatosteatosis progressing in HFD-fed mice cotreated with CLHs (Fig. 3A and B). Moreover, the biochemical blood markers related to liver damage, such as AST, ALT, and ALP values in HFD-fed mice, were decreased ($p < 0.05$) by supplementing with CLHs (Table 1). Furthermore, the highly expressed DGAT2 in livers of HFD-fed mice was reduced by supplementing with CLHs, which inferred that CLHs could retard the TG formation and lipid deposition (Fig. 3A–C & 4A). Moreover, the ACADM expressions in livers of HFD-fed mice were enhanced under CLH cotreatment (Fig. 4B). Overall, *in vivo* findings were consistent with the outcomes of the cell model (Figs. 2 and 4). In the previous studies, the hepatoprotection of L-leucine, L-lysine, L-ornithine, and L-aspartate in the manner of NAFLD had been mentioned; meanwhile, those lipid-lowering free amino acids (easily absorbed) existed in a plentiful amount in CLHs (Suppl. Table 2) [32-34].

Hepatic and peripheral IR (mainly skeletal muscle and white adipose tissue) were aggravated in all forms of NAFLD progression, gaining the risk of consecutive T2DM (Table 1) [6, 35]. For universal IR, the higher concentration of circulating glucose and FFA both stimulated an elevation of *de novo* lipogenesis (DNL) in the liver, which represents a key feature of NAFLD (Table 1 & Fig. 3A) [7]. In recent reports, dietary leucine was considered a key player in the insulin-sensitivity improvement, which might also manipulate both the glucose and lipid metabolism while there was 831.75 ± 0.83 mg leucine per 100g CLHs (Suppl. Table 2) [15]. According to the results (Fig. 3E), CLH supplementation sustained the insulin signal sensitivity in skeletal muscle and peri-renal fat tissues against the long-term HFD feeding because of the downstream GLUT4 response to upstream insulin signal in CLH cotreated mice compared to that of HFD group. Kairupan et al. reported that expressions of GLUT4 were modulated by upstream AMPK signal in skeletal muscle, which was consistent to our results [36]. Graham et al. proposed that the amount of GLUT4 in white adipose tissues represented a good systemic insulin sensitivity marker [37]. These effects might also contribute to decreased fasted serum glucose and FFA. Therefore, the DNL might remain non-activated in hepatic tissue due to a lack of external factors and resources. *In vitro* (ACC & FAS) and *in vivo* (DGAT2) results in this study conformed to this assumption (Figs. 2 & 4A).

Hepatosteatosis was aggravated because of the loss of mitochondrial adaption [38, 39]. Since metabolic burdens of dietary fat exist, hepatic mitochondria transiently adapt to lipid availability enhancement by upregulating their oxidative capacity at the expense of decreased coupling efficiency [39]. Loss of mitochondria adaptation caused lipid overloading, oxidative stress, and inflammation, resulting in non-alcoholic steatohepatitis [7]. The results of ACADM expressions indicate that CLH supplementation promoted mitochondrial fatty-acid β oxidation. The CPT1 and UCP2 were upregulated in CLH-treated cells (Figs. 2 & 4B), which sustain the mitochondrial adaption. Likewise, BCAAs (especially leucine) modulation on mitochondrial biogenesis and fatty-acid β oxidation through the AMPK dependent pathway were revealed [40]. Furthermore, the antioxidant effects of CLHs had been mentioned [2, 21, 31]. In this study, CLH supplementation also showed an increase of antioxidant capacities and a decrease of inflammatory responses in livers of HFD-fed mice (Table 1). Overall, mitochondrial adaption and function were sustained via supplementing with CLHs.

The fatty-acid β oxidation was the crucial mitochondrial function in lipid metabolism. Its major product was the β-hydroxybutyrate (a major component of KB). In this study, CLH enhanced the fatty-acid β oxidation flux (Figs. 2 & 4B); remarkably, the serum KB value of the CLH group was even higher ($p < 0.05$) than that of the Control group

(Table 1). Although the universal IR would suppress the fatty-acid β oxidation flux, the CLH supplementation showed an increased tendency toward serum KB with a dose-dependent effect (Table 1). Moreover, the KB results correspond to the results of ACADM expression (Table 1 & Fig. 4B). Xu et al. proclaimed that ketogenic essential amino acids (leucine and lysine) ameliorated hepatosteatosis; meanwhile, diabetic ketoacidosis was crucial for clinical diagnosis [41]. The serum β-hydroxybutyrate of diabetic mice could be elevated almost 10-times of those of normal mice (2 mg/dL vs. 19-20 mg/dL) [42, 43]. However, ketosis but no ketoacidosis in mice was observed under 20-week CLH-supplementation in this study.

In conclusion, bio-active free amino acids were a major constituent of CLHs, including L-lysine, BCAAs, β-alanine, L-aspartic acid, glycine, L-ornithine, and taurine, as well as anserine. Through the OA-induced cellular steatosis and HFD-induced mouse model, the attenuative effects of CLHs on hepatic lipid deposition, hepatic/peripheral IR, and oxidative stress have been elucidated (Fig. 5). CLH supplementation could improve the universal glucose homeostasis via sustaining hepatic and peripheral insulin sensitivities and improved lipid dyshomeostasis to demonstrate anti-IR, anti-hepatosteatosis, and anti-obesity in various outcomes. To sum up, this CLH development could not only enhance the added value of broiler livers as the nutraceutical ingredients in the niche market but also decrease the environmental burden caused by the broiler industry.

Acknowledgments

We acknowledge funding for this research from the Ministry of Science and Technology, Taiwan (Project: MOST 106-2313-B-002-040-MY3 and MOST 109-2313-B-002-007-MY3) and Council of Agriculture, Executive Yuan, Taiwan (Project: 107AS-15.4.1-ST-a5, 108AS-14.1.1-ST-a2, and 109AS-12.1.1-ST-a1).

Suppl. Table 2. Proximate analysis, free amino acid composition, and imidazole-ring dipeptides of chicken-liver hydrolysates.

	CLHs
Nutrient (per 100 gram)	
Water (g)	6.82 ± 0.09
Crude protein (g)	69.57 ± 0.00
Crude fat (g)	0.14 ± 0.01
Ash (g)	22.93 ± 0.92
Amino acids (mg/100g dried weight)	
L-Arginine	605.88 ± 10.50
L-Histidine	196.64 ± 6.03
L-Isoleucine	380.54 ± 20.53
L-Leucine	831.75 ± 0.83
L-Lysine	776.61 ± 7,57
L-Methionine	295.15 ± 24.55
L-Phenylalanine	422.66 ± 52.78
L-Threonine	470.95 ± 6.85
Tryptophan	74.26 ± 4.00
L-Valine	626.49 ± 12.74
Total EAA	4680.92 ± 102.53
Total BCAA	1838.78 ± 33.27
L-Alanine	780.03 ± 4.37
β-Alanine	31.73 ± 0.75
γ-Aminobutyric acid	1.87 ± 0.00
DL-3-Aminoisobutyric acid	23.23 ± 7.03
Asparagine	23.11 ± 2.59
L-Aspartic acid	710.31 ± 17.52
L-Cystathionine	21.33 ± 1.92
Ethanolamine	18.60 ± 1.65
L-Glutamic acid	1400.50 ± 135.48
Glycine	438.24 ± 3.96
DL-plus allo-δ-Hydroxylysine	5.81 ± 0.28
L-Hydroxyproline	24.56 ± 1.04
L-Ornithine	36.84 ± 5.55
O-phosphoserine	63.41 ± 6.11
L-Proline	612.19 ± 11.37
L-Serine	598.25 ± 9.79
Taurine	301.09 ± 29.64
L-Tyrosine	335.74 ± 16.89
Total NEAA	5426.83 ± 184.35
L-Anserine	123.79 ± 1.29
L-Carnosine	N.D.
Imidazole-ring dipeptide	123.79 ± 1.29

*EAA: essential amino acid; BCAA: branched-chain amino acid; NEAA: non-essential amino acid; N. D.: not detectible.

Appendix A. Supplementary material

Suppl. Table 1. List of antibodies for western bolting in this study.

Target protein	Abbr. name	Brand	Catalog NO.	Dilution
acetyl-CoA carboxylase	ACC	Cell Signaling Technology Inc.	#3662	1:1000
fatty acid synthase	FAS	Cell Signaling Technology Inc.	#3180	1:1000
AMP-activated protein kinase α	AMPKα	Cell Signaling Technology Inc.	#2532	1:1000
phosphorylated AMP-activated protein kinase α	p-AMPKα	Cell Signaling Technology Inc.	#2535	1:1000
carnitine palmitoyltransferase I	CPT1	Millipore Co.	#ABS65	1:1000
peroxisome proliferator-activated receptor α	PPARα	Abcam	ab24509	1:1000
uncoupling proteins 2	UCP2	Millipore Co.	#662047	1:1000
insulin receptor	IRβ	Cell Signaling Technology Inc.	#3025	1:1000
glucose transporter type 4	GLUT4	Cell Signaling Technology Inc.	#2213	1:1000
β-Tubulin	β-Tubulin	Cell Signaling Technology Inc.	#2128	1:1000

References

[1] Council of Agriculture, Executive Yuan, Taiwan. Agricultural Production: 2. Livestock Production; 2020. Available at https://eng.coa.gov.tw/ws.php?id=2505611. [Accessed 17 November 2020].

[2] Yang KT, Lin C, Liu CW, Chen YC. Effects of chicken-liver hydrolysates on lipid metabolism in a high-fat diet. Food Chem 2014;160:148–56.

[3] Lin YL, Tai SY, Chen JW, Chou CH, Fu SG, Chen YC. Ameliorative effects of pepsin-digested chicken liver hydrolysates on development of alcoholic fatty livers in mice. Food Funct 2017;8:1763–74.

[4] Chen YC, Chen PJ, Tai SY. National Taiwan University, US10105; 2018, 400B2.

[5] International Diabetes Federation (IDF). Global picture. IDF diabetes atlas. 9th ed. Brussels, Belgium: IDF; 2019.

[6] Gaggini M, Morelli M, Buzzigoli E, DeFronzo RA, Bugianesi E, Gastaldelli A. Non-alcoholic fatty liver disease (NAFLD) and its connection with insulin resistance, dyslipidemia, atherosclerosis and coronary heart disease. Nutrients 2013;5:1544–60.

[7] Tilg H, Moschen AR, Roden M. NAFLD and diabetes mellitus. Nat Rev Gastroenterol 2017;14:32–42.

[8] European Association for the Study of the Liver (EASL), European Association for the Study of Diabetes (EASD), European Association for the Study of Obesity (EASO). EASL-EASD-EASO Clinical Practice Guidelines for the management of non-alcoholic fatty liver disease. J Hepatol 2016;64:1388–402.

[9] Liu Y, Wang D, Zhang D, Lv Y, Wei Y, Wu W, et al. Inhibitory effect of blueberry polyphenolic compounds on oleic acid-induced hepatic steatosis in vitro. J Agric Food Chem 2011;59:12254–63.

[10] Drummond E, Flynn S, Whelan H, Nongonierma AB, Holton TA, Robinson A, et al. Casein hydrolysate with glycemic control properties: Evidence from cells, animal models, and humans. J Agric Food Chem 2018;66:4352–63.

[11] Yang Y, Wang J, Zhang Y, Li J, Sun W. Black sesame seeds ethanol extract ameliorates hepatic lipid accumulation, oxidative stress, and insulin resistance in fructose-induced nonalcoholic fatty liver disease. J Agric Food Chem 2018;66:10458–69.

[12] Sulochana KN, Punitham R, Ramakrishnan S. Beneficial effect of lysine and amino acids on cataractogenesis in experimental diabetes through possible antiglycation of lens proteins. Exp Eye Res 1998;67:597–601.

[13] Li W, Zhang Y, Shao N. Protective effect of glycine in streptozotocin-induced diabetic cataract through reductase inhibitory activity. Biomed Pharmacother 2019;114:108794.

[14] Nandhini AT, Thirunavukkarasu V, Anuradha CV. Taurine prevents collagen abnormalities in high fructose-fed rats. Indian J Med Res 2005;122:171–7.

[15] Bruckbauer A, Zemel MB, Thorpe T, Akula MR, Stuckey AC, Osborne D, et al. Synergistic effects of leucine and resveratrol on insulin sensitivity and fat metabolism in adipocytes and mice. Nutr Metab 2012;9:77.

[16] Chang JJ, Hsu MJ, Huang HP, Chung DJ, Chang YC, Wang CJ. Mulberry anthocyanins inhibit oleic acid-induced lipid accumulation by reduction of lipogenesis and promotion of hepatic lipid clearance. J Agric Food Chem 2013;61:6069–76.

[17] Samuel VT, Shulman GI. The pathogenesis of insulin resistance: integrating signaling pathways and substrate flux. J Clin Investig 2016;126:12–22.

[18] Chang R, Chou MC, Hung LY, Wang ME, Hsu MC, Chiu CH. Study of valproic acid-enhanced hepatocyte steatosis. Biomed Res Int 2016;2016:9576503.

[19] Lau JKC, Zhang X, Yu J. Animal models of non-alcoholic fatty liver disease: current perspectives and recent advances. J Pathol 2017;241:36–44.

[20] Association of Official Analytical Chemists (AOAC). Official Methods of Analysis. 2005. Arlington, VA, USA.

[21] Wu YS, Lin YL, Huang C, Chiu CH, Nakthong S, Chen YC. Cardiac protection of functional chicken-liver hydrolysates on the high-fat diet-induced cardio-renal damages via sustaining autophagy homeostasis. J Sci Food Agric 2020;100:2443–52.

[22] Chang YY, Lin YL, Yang DJ, Liu CW, Hsu CL, Tzang BS, et al. Hepatoprotection of noni juice against chronic alcohol consumption: Lipid homeostasis, antioxidation, alcohol clearance, and anti-inflammation. J Agric Food Chem 2013;61:11016–24.

[23] Chen PJ, Tseng JK, Lin YL, Wu YS, Hsiao YT, Chen JW, et al. Protective effects of functional chicken liver hydrolysates against liver fibrogenesis: antioxidation, anti-inflammation, and antifibrosis. J Agric Food Chem 2017;65:4961–9.

[24] Dixon JB, Bhathal PS, Hughes NR, O'Brien PE. Nonalcoholic fatty liver disease: Improvement in liver histological analysis with weight loss. Hepatology 2004;39:1647–54.

[25] Andrikopoulos S, Blair AR, Deluca N, Fam C, Proietto J. Evaluating the glucose tolerance test in mice. Am J Physiol Endocrinol Metab 2008;295:E1323–32.

[26] Chen JW, Kong ZL, Tsai ML, Lo CY, Ho CT, Lai CS. Tetrahydrocurcumin ameliorates free fatty acid-induced hepatic steatosis and improves insulin resistance in HepG2 cells. J Food Drug Anal 2018;26:1075–85.

[27] D'Antona G, Ragni M, Cardile A, Tedesco L, Dossena M, Bruttini F, et al. Branched-chain amino acid supplementation promotes survival and supports cardiac and skeletal muscle mitochondrial biogenesis in middle-aged mice. Cell Metab 2010;12:362–72.

[28] Peng X, Li J, Wang M, Qu K, Zhu H. A novel AMPK activator improves hepatic lipid metabolism and leukocyte trafficking in experimental hepatic steatosis. J Pharmacol Sci 2019;140:153–61.

[29] Yang TH, Yao HT, Chiang MT. Red algae (Gelidum amansii) got-water extract ameliorates lipid metabolism in hamsters fed a high-fat diet. J Food Drug Anal 2017;25:931–8.

[30] Tung YC, Liang ZR, Chou SF, Ho CT, Kuo YL, Cheng KC, et al. Fermented soy paste alleviates lipid accumulation in the liver by regulating the AMPK pathway and modulating gut microbiota in high-fat-diet-fed rats. J Agric Food Chem 2020;68:9345–57.

[31] Chou CH, Wang SY, Lin YT, Chen YC. Antioxidant activities of chicken liver hydrolysates by pepsin treatment. Int J Food Sci Technol 2014;49:1654–62.

[32] Lin HY, Chen CC, Chen YJ, Lin YY, Mersmann HJ, Ding ST. Enhanced amelioration of high-fat diet-induced fatty liver by docosahexaenoic acid and lysine supplementations. Biomed Res Int 2014;2014:310981.

[33] Pedroso JA, Zampieri TT, JJr Donato. Reviewing the effects of L-leucine supplementation in the regulation of food intake, energy balance, and glucose homeostasis. Nutrients 2015;7:3914–37.

[34] Butterworth RF, Canbay A. Hepatoprotection by L-ornithine L-aspartate in non-alcoholic fatty liver disease. Dig Dis 2019;37:63–8.

[35] Bugianesi E, Gastaldelli A, Vanni E, Gambino R, Cassader M, Baldi S, et al. Insulin resistance in non-diabetic patients with non-alcoholic fatty liver disease: sites and mechanisms. Diabetologia 2005;48:634–42.

[36] Kairupan TS, Cheng KC, Asakawa A, Amitani H, Yagi T, Ataka K, et al. Rubiscolin-6 activates opioid receptors to enhance glucose uptake in skeletal muscle. J Food Drug Anal 2019;27:266–74.

[37] Graham TE, Yang Q, Blüher M, Hammarstedt A, Ciaraldi TP, Henry RR, et al. Retinol-binding protein 4 and insulin resistance in lean, obese, and diabetic subjects. N Engl J Med 2006;354:2552–63.

[38] Li Z, Li Y, Zhang HX, Guo JR, Lam C, Wang CY, et al. Mitochondria-mediated pathogenesis and therapeutics for non-alcoholic fatty liver disease. Mol Nutr Food Res 2019;63:e1900043.

[39] Koliaki C, Szendroedi J, Kaul K, Jelenik T, Nowotny P, Jankowiak F, et al. Adaptation of hepatic mitochondrial function in humans with non-alcoholic fatty liver is lost in steatohepatitis. Cell Metab 2015;21:739–46.
[40] Sun X, Zemel MB. Leucine modulation of mitochondrial mass and oxygen consumption in skeletal muscle cells and adipocytes. Nutr Metab 2009;6:26.
[41] Xu L, Kanasaki M, He J, Kitada M, Nagao K, Jinzu H, et al. Ketogenic essential amino acids replacement diet ameliorated hepatosteatosis with altering autophagy-associated molecules. Biochim Biophys Acta 2013;1832:1605–12.
[42] Denroche HC, Levi J, Wideman RD, Sequeira RM, Huynh FK, Covey SD, et al. Leptin therapy reverses hyperglycemia in mice with streptozotocin-induced diabetes, independent of hepatic leptin signaling. Diabetes 2011;60:1414–23.
[43] Trak-Smayra V, Paradis V, Massart J, Nasser S, Jebara V, Fromenty B. Pathology of the liver in obese and diabetic ob/ob and db/db mice fed a standard or high-calorie diet. Int J Exp Pathol 2011;92:413–21.